Supplementary Information

Dual role of N-doped graphene film as cathode material for anodic organic oxidation and persulfate production and as planar carbocatalyst for non-electrochemical persulfate activation

Eun-Tae Yun,[a] Woonghee Lee,[b] Yong-Yoon Ahn,[c] Jaemin Choi,[a] John D. Fortner,[d] Kangwoo Cho,[b] Seungkwan Hong*,[a] Jaesang Lee*,[a]

[a] Civil, Environmental, and Architectural Engineering, Korea University, Seoul 136-701, Korea

[b] Environmental Science and Engineering, Pohang University of Science and Technology (POSTECH), Pohang 37673, Korea

[c] Korea Polar Research Institute (KOPRI), Incheon 21990, Republic of Korea

[d] Chemical and Environmental Engineering, Yale University, New Haven, CT, 06520, United States

Submitted to

Environmental Science: Nano

*Corresponding author.

Phone: +82-2-3290-4864; fax: +82-2-928-7656; E-mail: lee39@korea.ac.kr (J.Lee)

Phone: +82-2-3290-3322; fax: +82-2-3290-5999; E-mail: skhong21@korea.ac.kr (S.Hong)

Table S1. LC-MS identification of intermediates generated during 4-CP degradation in the electrochemical system equipped with BDD as the anode and NG/NF as the cathode during two separate on and off periods (current density = 90 mA/cm^2; $[4\text{-CP}]_0$ = 0.2 mM (switch-on) or 0.1 mM (switch-off); $[Na_2SO_4]_0$ = 100 mM; pH_i = 5).

Compounds	Molecular formula	Retention time (min)	m/z	Mass error (ppm)	On	Off
4-Chlorophenol	C_6H_4ClO	10.27	126.9960	0.44	O[a]	O
Benzoquinone	$C_6H_3O_2$	4.4	108.0204	N/A[b]	O	O
Hydroquinone	$C_6H_5O_2$	2.12	108.0204	N/A[b]	O	O
Maleic (or Fumaric) acid	$C_4H_3O_4$	1.28	115.0024	-1.71	O	O
Succinic acid	$C_4H_5O_4$	1.43	117.0181	-1.57	O	O
Hydroxybenzoquinone	$C_6H_3O_3$	12.37	123.0075	-0.77	X[c]	O
2,5-Dihydroxy-1,4-benzoquinone	$C_6H_3O_4$	1.28	139.0026	0.17	O	X
1,2,4,5-Benzenetetrol	$C_6H_5O_4$	6.26	141.0182	-0.44	O	X
4-Chlorocatechol	$C_6H_4ClO_2$	8.56	142.9893	-0.59	X	O
Chloro-maleic (or -fumric) acid	$C_4H_2ClO_4$	1.60	148.9636	-0.14	O	O
4-Chloro-5-hydroxy-1,2,-benzoquinone	$C_6H_2ClO_3$	6.66	156.9689	1.40	X	O
Dichlorophenyl-diol	$C_{12}H_7Cl_2O_2$	11.97	252.9828	4.18	O	O

[a]: detected
[b]: not available
[c]: not detected

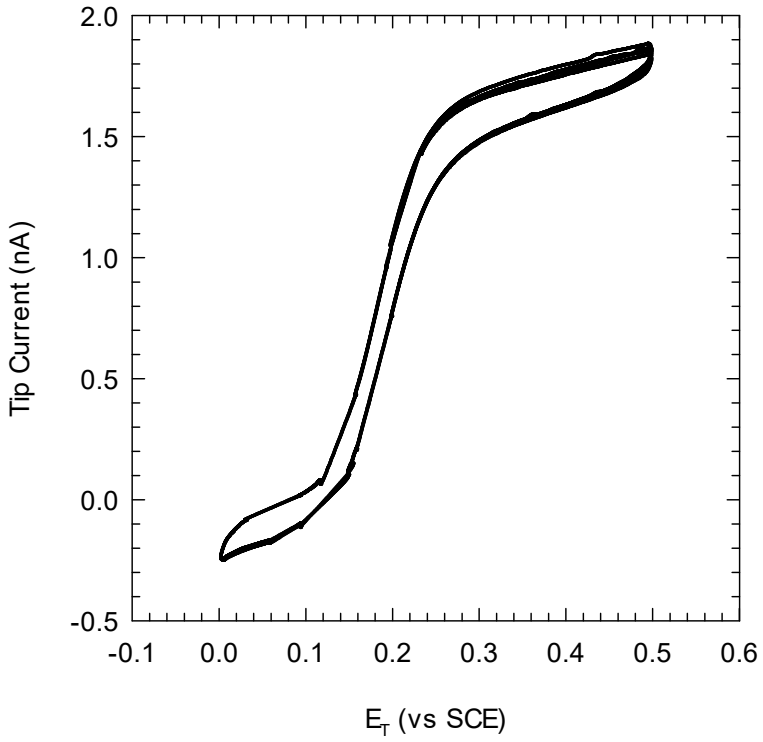

Figure S1. Cyclic voltammograms for Pt UME tip in 1 mM FcMeOH + 100 mM KCl (scan rate of 50 mV/s) to rationalize a diffusion limited tip current at +0.35 V_{SCE} (+0.241 V_{NHE}) for FcMeOH oxidation.

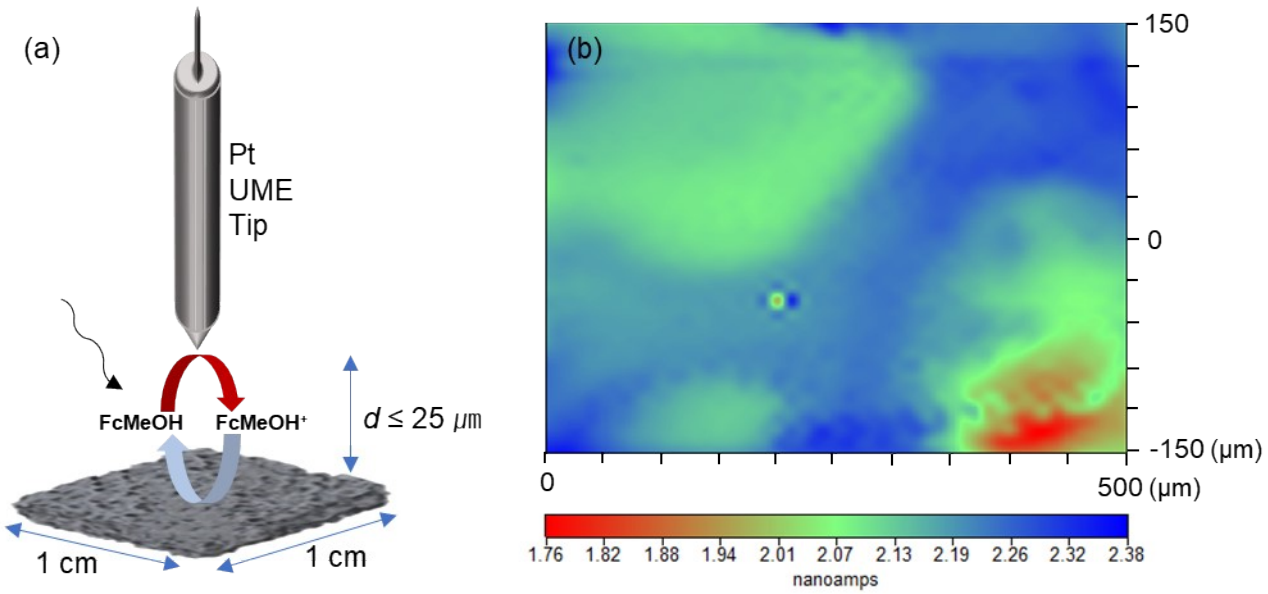

Figure S2. (a) A schematic diagram for feedback mode of SECM and (b) a representative SECM areal scan image of G/NF sample (1 × 1 cm^2) in 1 mM FcMeOH + 100 mM KCl (applied bias = +0.241 V_{NHE}; scan velocity = 100 μm/s; step size = 10 μm/point; tip-to-substrate distance = 25 μm; under open circuit condition).

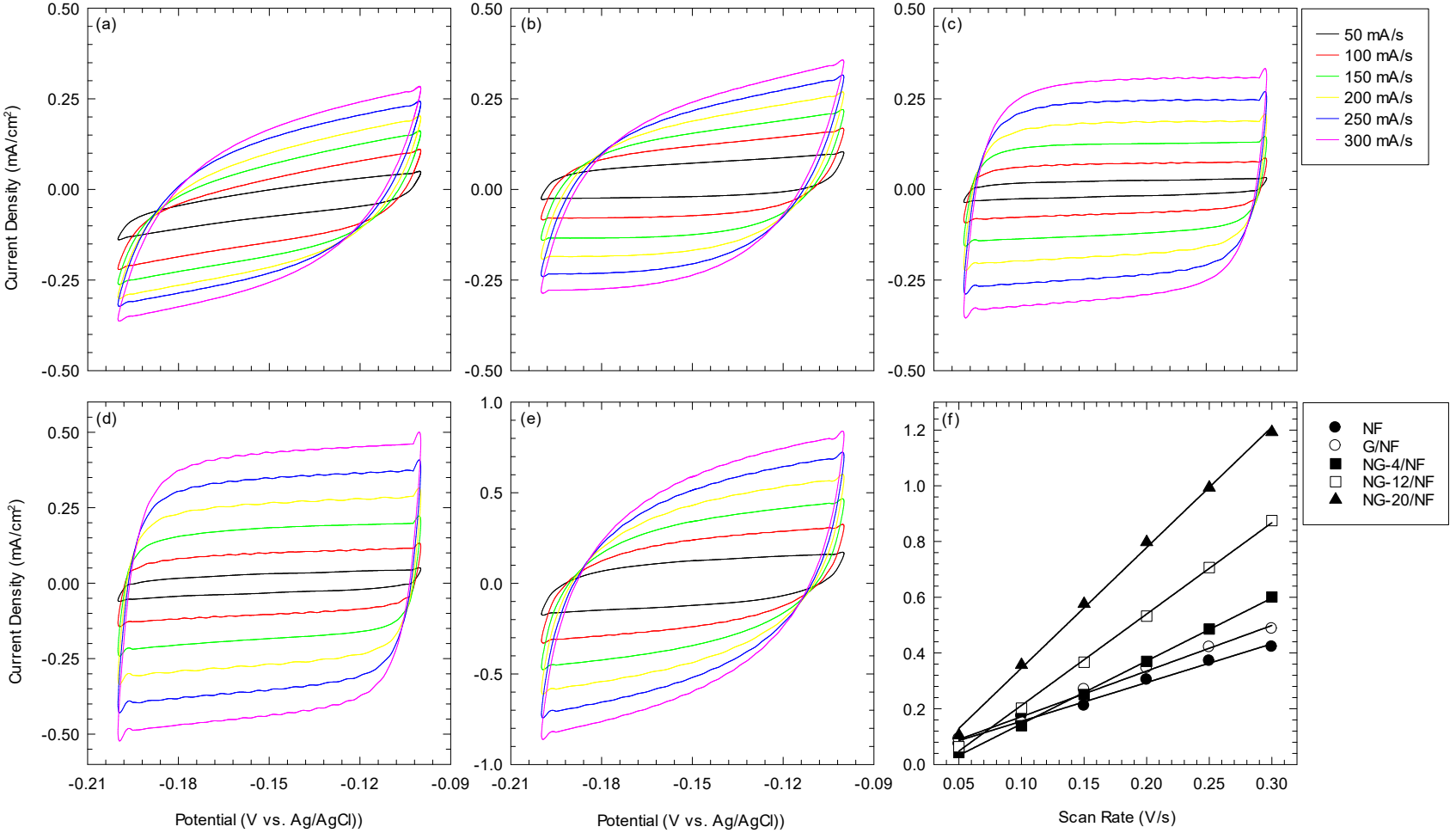

Figure S3. Cyclic voltammetries of (a) NF, (b) G/NF, (c) NG-4/NF, (d) NG-12/NF, (e) NG-20/NF, and (f) plots of current density versus scan rate.

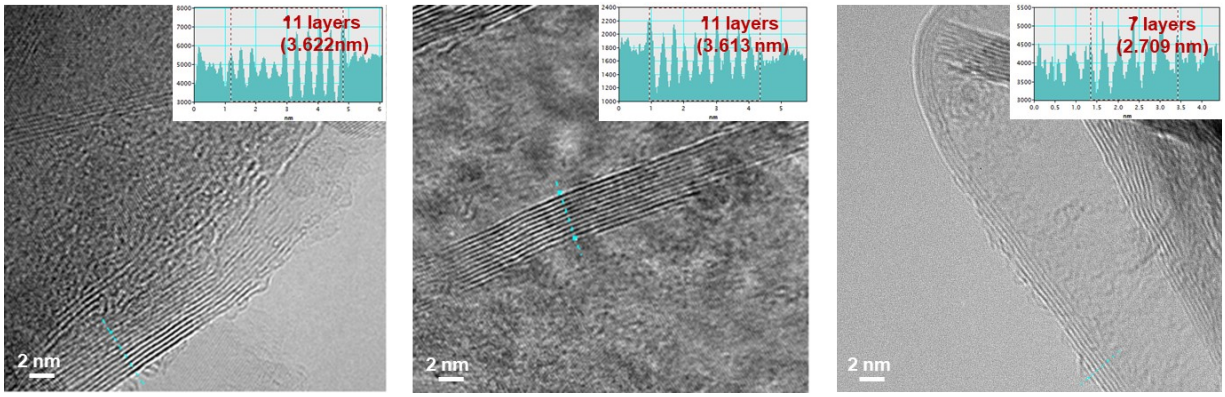

Figure S4. TEM images of NG-20 with the layer number of 7 to 11.

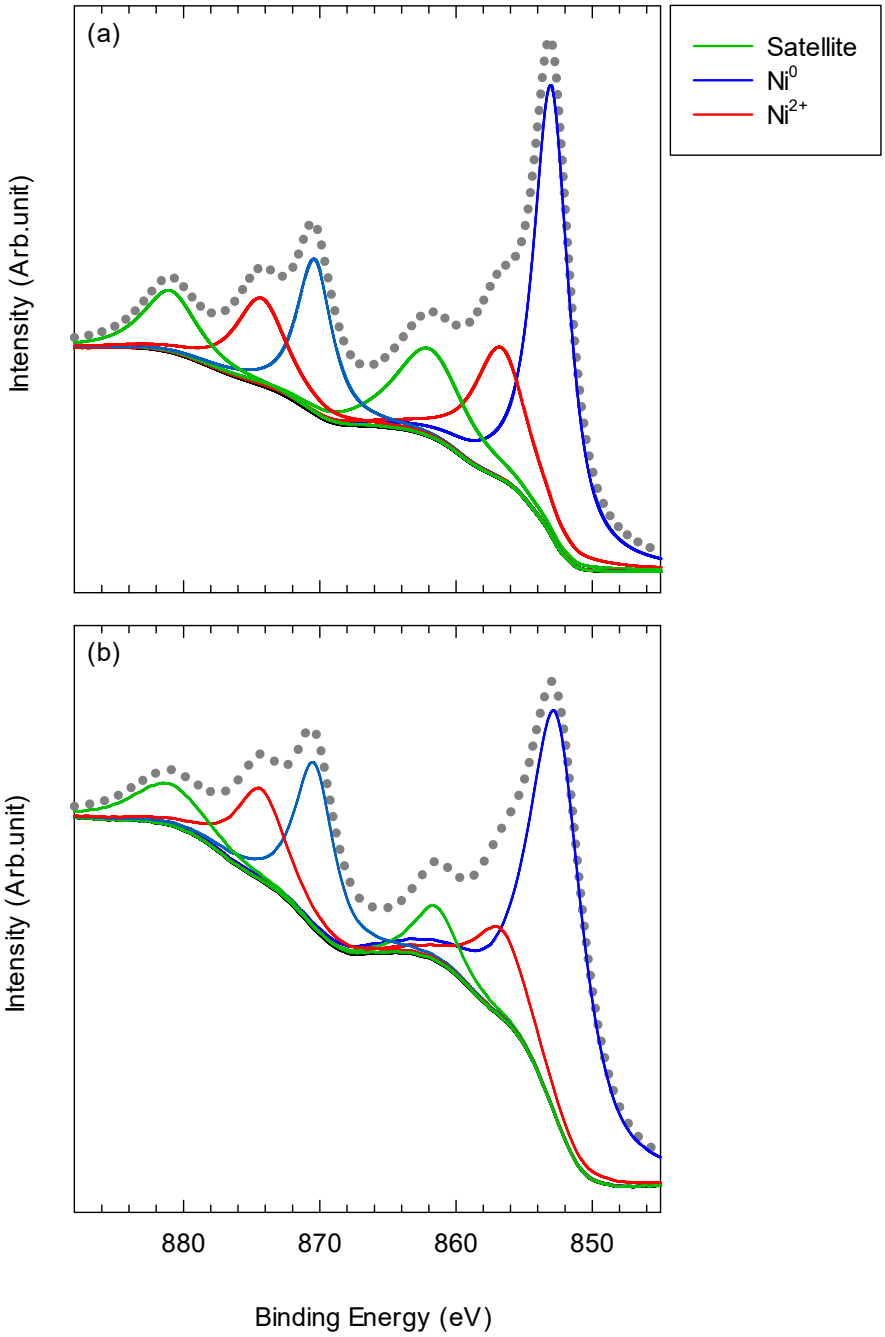

Figure S5. Ni2p XPS spectra of (a) pristine NF and (b) heat-treated NF in NH_3 flow.

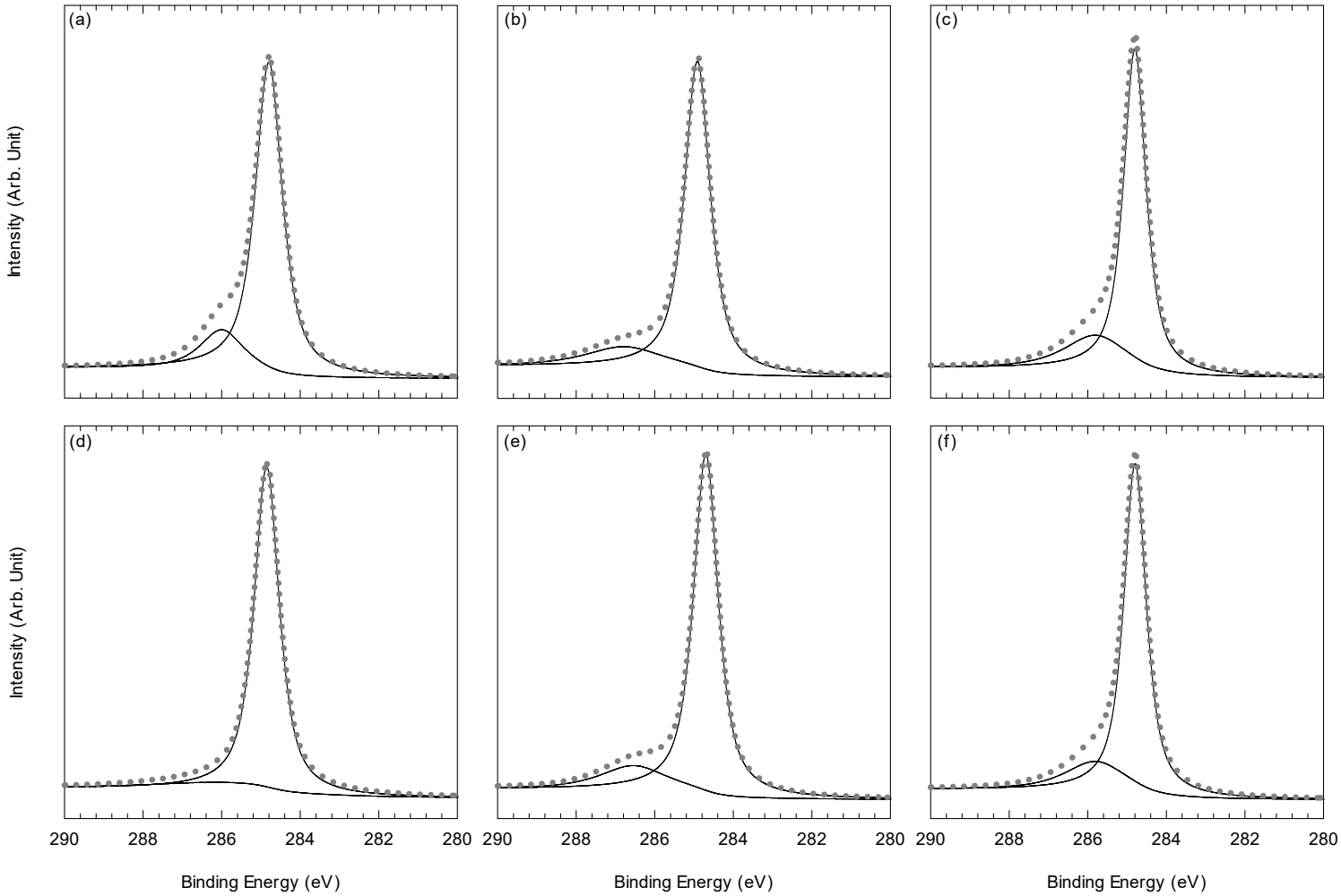

Figure S6. C1s XPS spectra of (a) NG-2/NF, (b) NG-4/NF, (c) NG-8/NF, (d) NG-12/NF, (e) NG-16/NF, and (f) NG-20/NF.

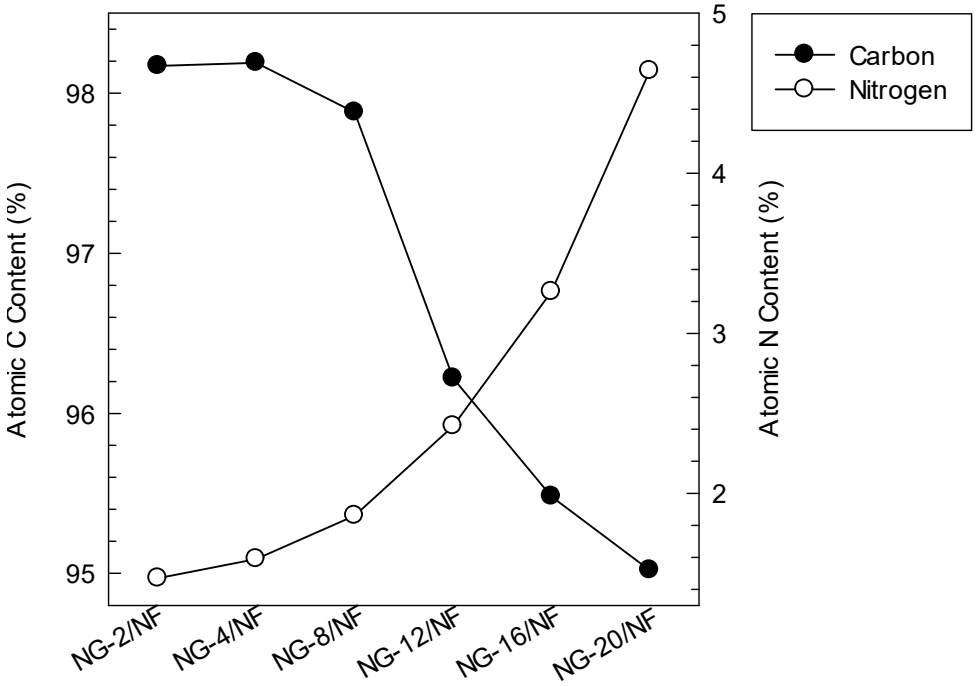

Figure S7. Surface atomic percentages of carbon and nitrogen in the N-doped graphene samples prepared under varying NH_3 flow conditions.

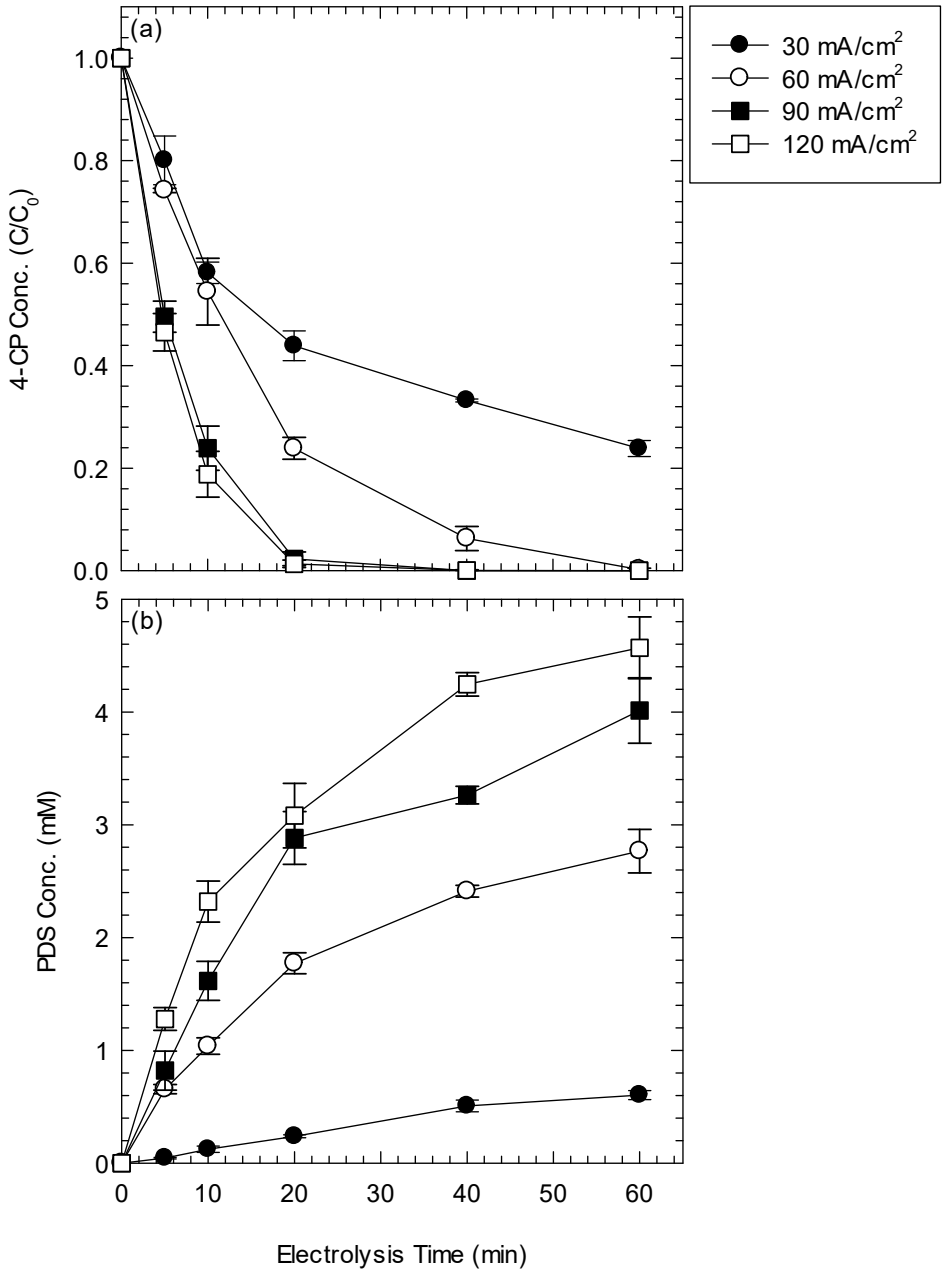

Figure S8. Anodic (a) 4-CP degradation and (b) PDS production under varying current density conditions ($[4\text{-CP}]_0$ = 0.2 mM; $[Na_2SO_4]_0$ = 100 mM; pH_i = 5).

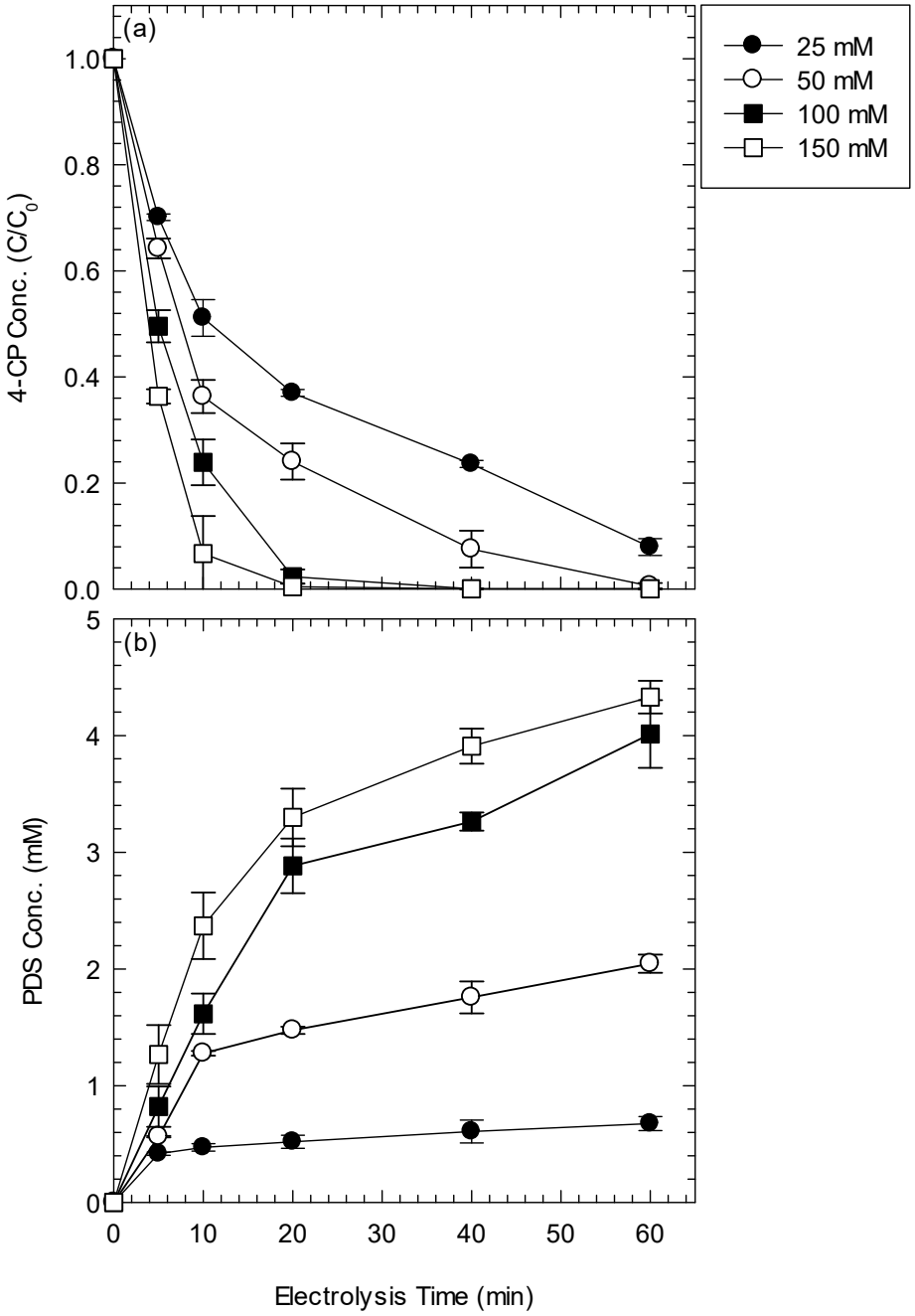

Figure S9. Anodic (a) 4-CP degradation and (b) PDS production under varying SO_4^{2-} electrolyte concentration conditions (current density = 90 mA/cm^2; $[4\text{-CP}]_0$ = 0.2 mM; pH_i = 5).

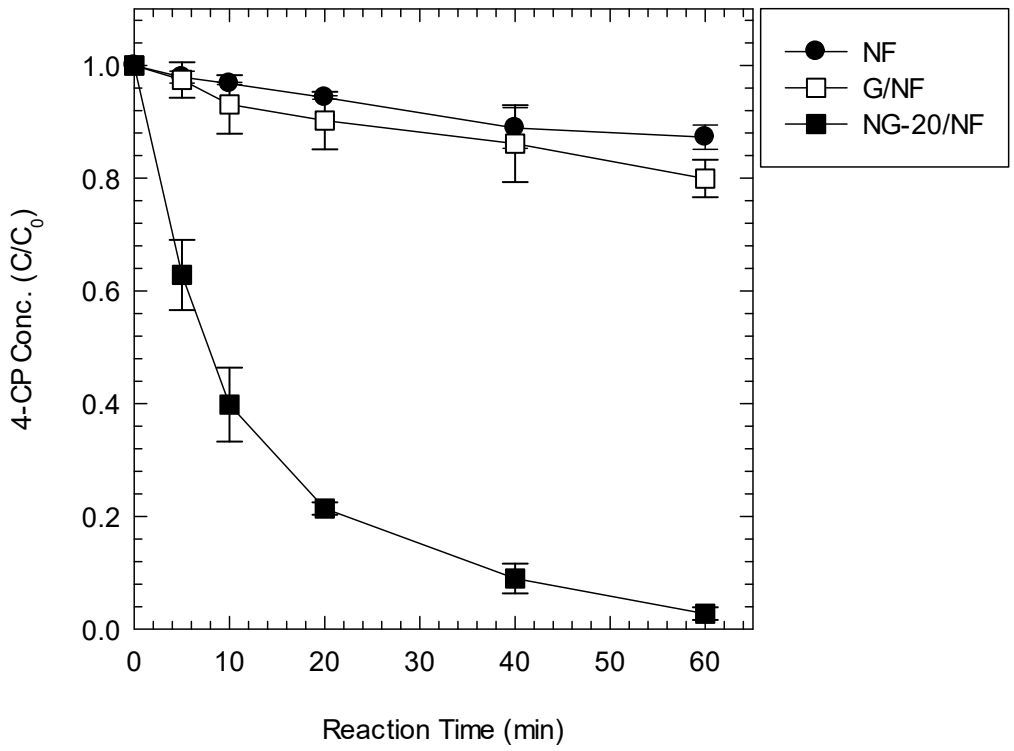

Figure S10. 4-CP degradation during PDS activation by NF, G/NF, and NG-20/NF ($[PDS]_0$ = 5 mM; $[4\text{-CP}]_0$ = 0.1 mM; pH_i = 5).

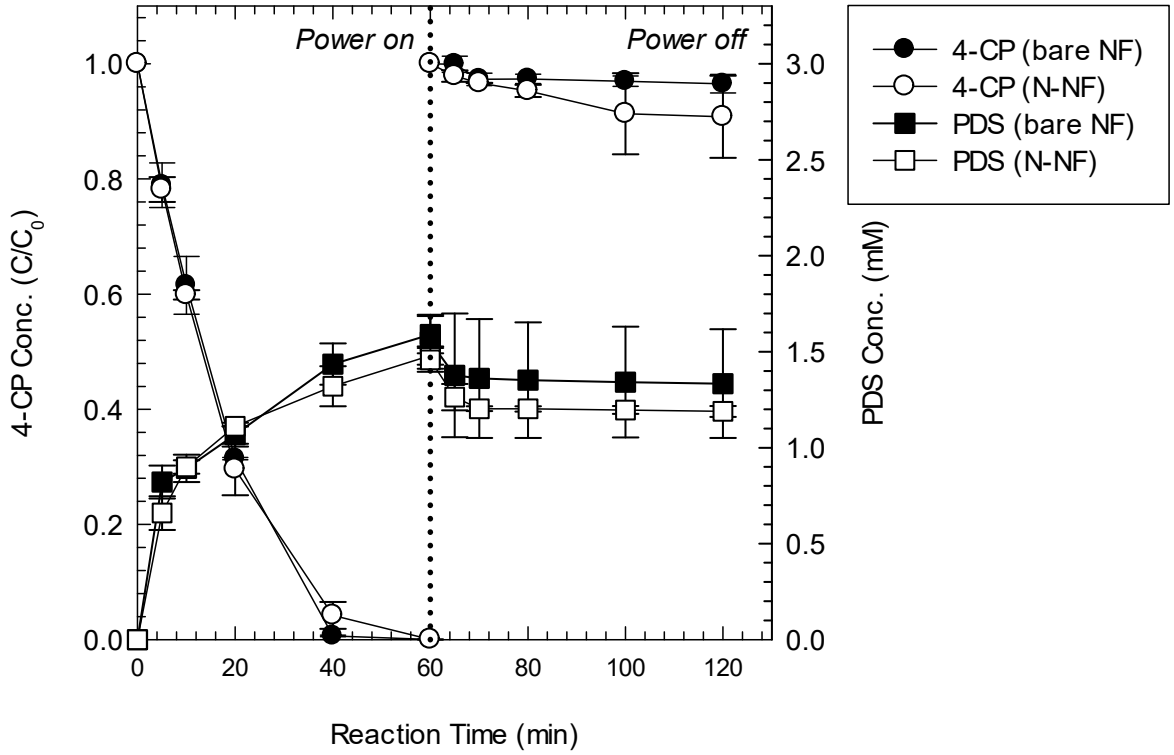

Figure S11. Time-dependent changes in 4-CP and PDS concentrations in the electrochemical systems equipped with BDD as the anode and bare NF and N-NF as the cathode during two separate on and off periods (current density = 90 mA/cm^2; $[4\text{-CP}]_0$ = 0.2 mM (switch-on) or 0.1 mM (switch-off); $[Na_2SO_4]_0$ = 100 mM; pH_i = 5).

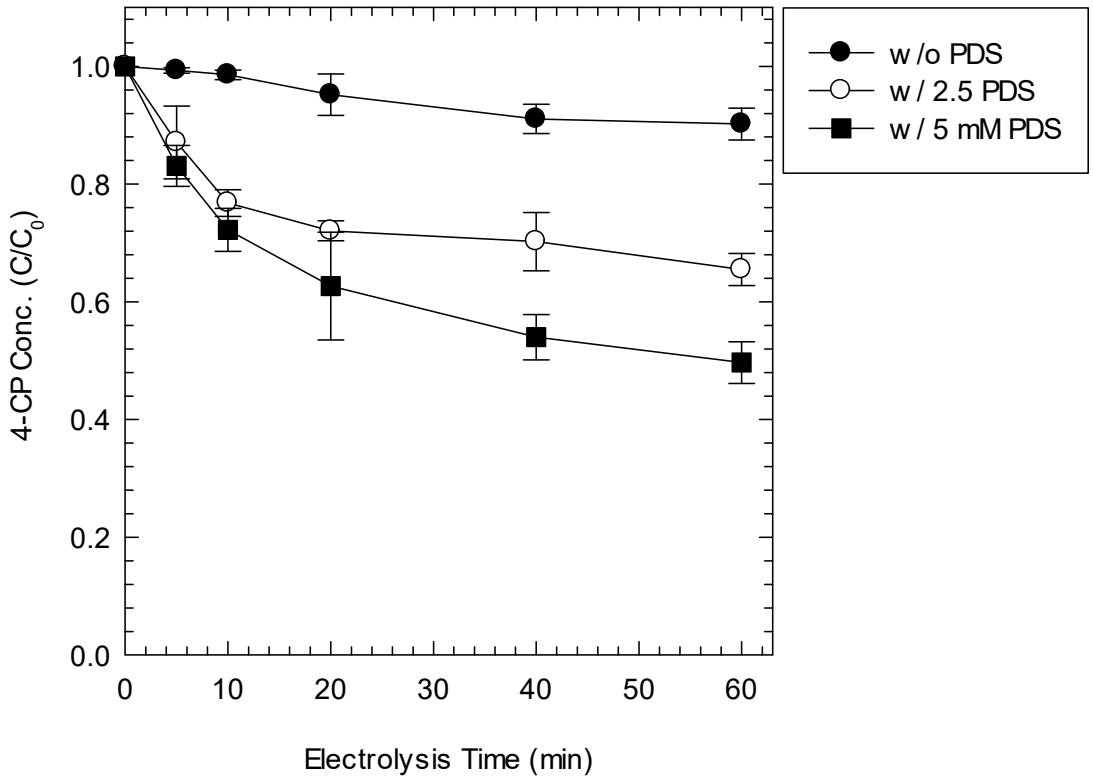

Figure S12. 4-CP degradation via cathodic PDS activation on NG-20/NF (current density = 90 mA/cm^2; $[4\text{-CP}]_0$ = 0.2 mM; $[Na_2SO_4]_0$ = 100 mM; pH_i = 5).

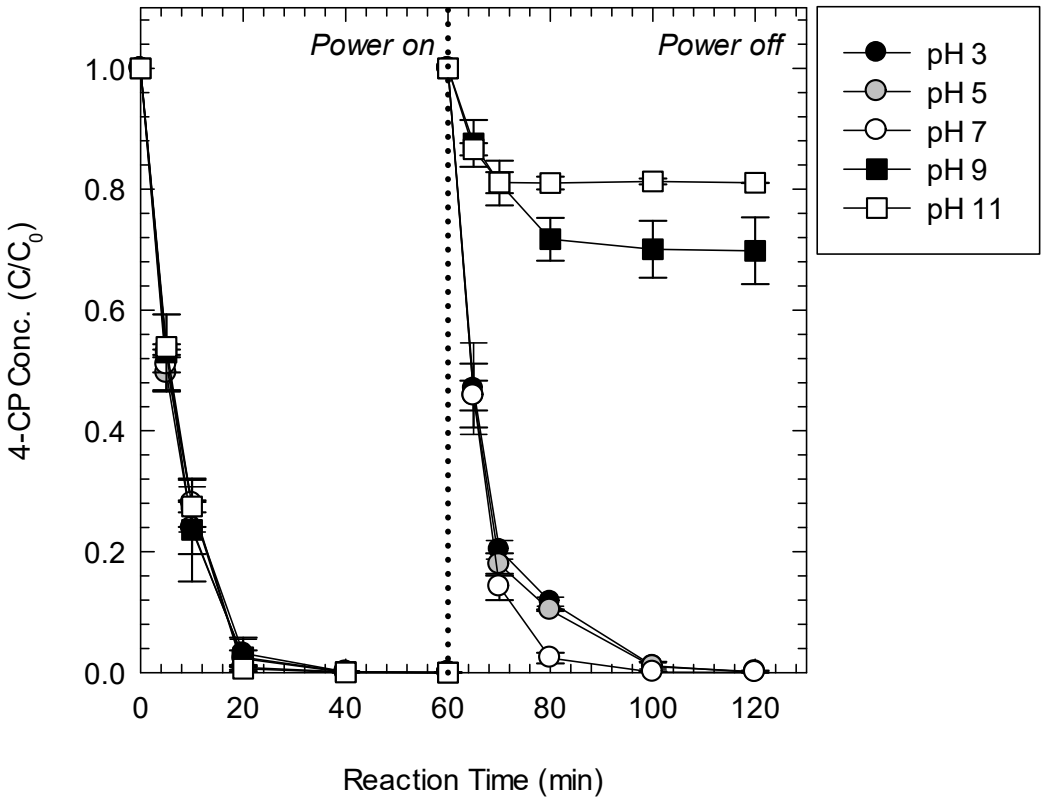

Figure S13. Effect of pH on the rate of 4-CP degradation via anodic oxidation and carbocatalytic PDS activation in the electrochemical systems equipped with BDD as the anode and NG-20/NF as the cathode during two separate on and off periods (current density = 90 mA/cm^2; $[4\text{-CP}]_0$ = 0.2 mM (switch-on) or 0.1 mM (switch-off); $[Na_2SO_4]_0$ = 100 mM).

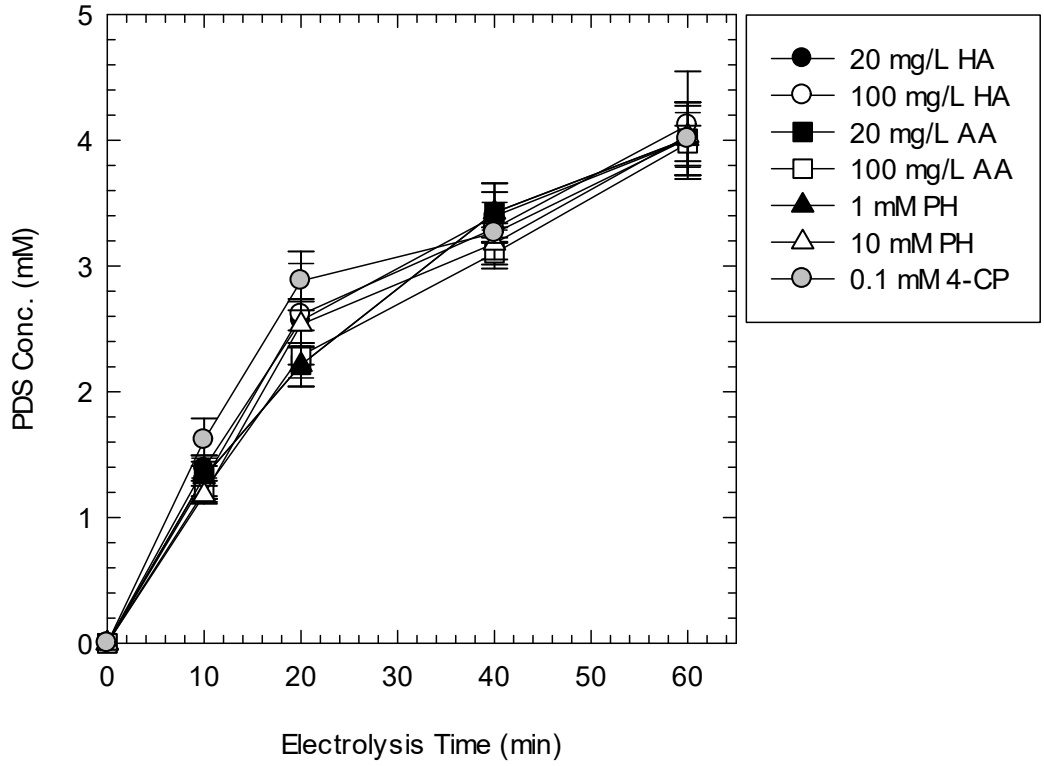

Figure S14. Anodic PDS production in the presence of humic acid (HA), alginic acid (AA), and phenol (current density = 90 mA/cm^2; $[Na_2SO_4]_0$ = 100 mM; pH_i = 5). NG-20/NF was used as the cathode.

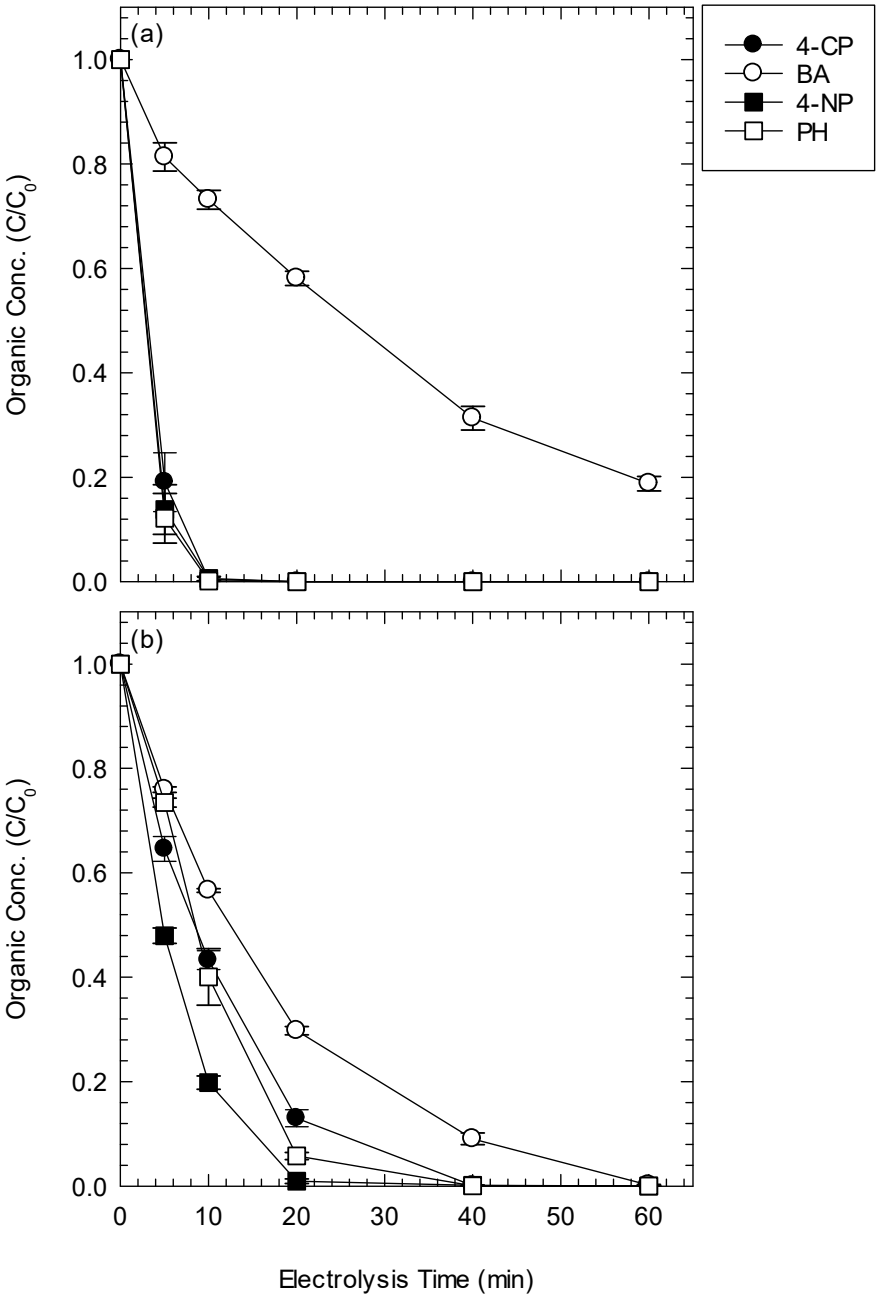

Figure S15. Anodic degradation of various organics, namely 4-CP, BA, 4-NP, and PH 4-CP in the electrochemical systems equipped with BDD and NG-20/NF as the anode and cathode, respectively, in the presence of (a) Cl^- and (b) ClO_4^- as electrolytes (current density = 90 mA/cm^2; $[organic\ compound]_0$ = 0.2 mM; $[NaCl]_0 = [NaClO_4]_0$ = 100 mM; pH_i = 5).